

A Dual Band Circularly Polarized Rectenna for RF Energy Harvesting Applications

Osama M. Dardeer^{1,2}, Hala A. Elsadek², Esmat A. Abdallah², and Hadia M. Elhennawy¹

¹Electronics and Electrical Communication Engineering Department
Ain Shams University, Cairo, Egypt
osamadardeer@eri.sci.eg, helhennawy@ieee.org

²Microstrip Department
Electronics Research Institute, Dokki, Giza, Egypt
hhelsadek92@gmail.com, esmataa2@hotmail.com

Abstract — This paper presents a dual band rectenna for RF energy harvesting applications. The receiving slot antenna has a single feed configuration with a coplanar waveguide (CPW) structure. A grounded-L strip is employed for circular polarized (CP) radiation. A stepped impedance matching stub is used to enhance the coupling between the feed line, inverted L-strip, and the slot. An asymmetric U-shaped strip is embedded near the upper right corner of the slot as a perturbed element. This asymmetric U-shaped strip is a key component to excite the required phase perturbation to produce a CP radiation. The antenna operates in the WiFi frequency bands of 2.45 GHz (IEEE 802.11b&g) and 5 GHz (IEEE 802.11a/h/j/n/ac/ax WLAN system). A dual band voltage doubler rectifier has been designed and implemented for RF to DC conversion. The impedance matching network for this rectifier is based on a Π -model dual band impedance transformer that is optimized to match two unequal complex loads at two operational frequencies.

Index Terms — Circular polarized antenna, dual band, rectenna, rectifier, RF energy harvesting, Π -model impedance transformer.

I. INTRODUCTION

The concept of allowing energy to flow between two points in space is a promising scheme in order to measure several physical quantities and benefit from these measures using suitable sensing devices, which will be powered by Wireless Power Transfer (WPT) scheme. This will increase the number of devices that can be powered simultaneously without the need for wired connections or even bulky batteries [1]. The power is transmitted in RF and then collected by a receiving antenna and converted to DC power using rectifier. This DC energy can be used as a source for low power devices or stored in storage devices as super capacitors, for

example. The combination between antenna and a rectifier is called a rectenna. Each harvesting node must contain a rectenna to capture the RF energy transmitted in space.

The rectenna is the key element in RF energy harvesting system. Circular polarized (CP) rectennas can be used due to the ability to obtain constant DC power at random polarization angles. In order to avoid the 3-dB polarization mismatch loss, Sun and Geyi in [2] proposed a dual linearly polarized receiving antenna and consequently dual feeding ports are required. In recent literature, different rectenna designs have been published for RF energy harvesting applications. These rectennas can operate in single band [2], dual band [3-7], and multiband [8-10]. Higher power conversion efficiency (PCE) can be obtained in narrow single band rectennas, but the amount of harvested RF power is low. On the other hand, multi-band rectennas suffer from lower PCE, but more harvested power. The challenge is to maximize the PCE for dual band or multi-band rectennas at the specific operating frequencies. Other trend is to present a broadband operation [11] in order to accumulate more RF power from different frequency bands.

In this paper, a dual band rectenna operating at 2.45 GHz ISM band and WLAN 5 GHz is proposed. The rectenna consists of a dual band CP slot antenna with coplanar waveguide (CPW) feed, and a dual band voltage doubler full wave rectifier. Each part of the rectenna is designed and tested separately, and then assembled in order to evaluate the overall performance. Both of the antenna and the rectifier have been fabricated on the standard FR4 substrate for cost reduction and ease of integration with the rest of the sensing circuitry. This paper is organized as follows: the design of the receiving antenna is presented in Section II. The design of the rectifier circuit is given in Section III. Section IV introduces the rectenna system performance, while Section V gives the conclusion.

II. RECEIVING ANTENNA DESIGN

The geometry of the proposed dual-band CP slot antenna with coplanar waveguide (CPW) feed is illustrated in Fig. 1. The antenna is fabricated on a square FR4 substrate with a dielectric constant of 4.3, thickness (h) of 1.6 mm, and loss tangent of 0.025. The antenna is fed by CPW line at the center of the structure. The CPW line has a 50 ohms characteristic impedance with a width W_f and a gap g_f . The size of the antenna is $54 \times 54 \text{ mm}^2$. A ring is formed by folding the ground plane, then a rectangular slot is subtracted from this ground to present the main radiating element of the proposed antenna. The slot dimensions are $30 \times 34 \text{ mm}^2$ which is designed to operate at 2.45 GHz. The A and L are optimized with A/L ratio of 1.588 in this study. The other dimensions of the antenna are listed in Table 1.

It is evident to note that there is a protruded tuning stub which is wider than the feed line. It may be considered as a stepped impedance section that greatly enhances the coupling between the feed line, inverted-L strip, and the slot. It also perturbs the magnetic current distribution in the slot so that the 3-dB axial ratio band would be adjusted. An inverted-L strip at the upper left corner of the slot contributes to the circular polarized radiation of the antenna [12]. This grounded L strip should be square ($14 \text{ mm} \times 14 \text{ mm}$) in order to enhance the axial ratio bandwidth for the lower resonant frequency.

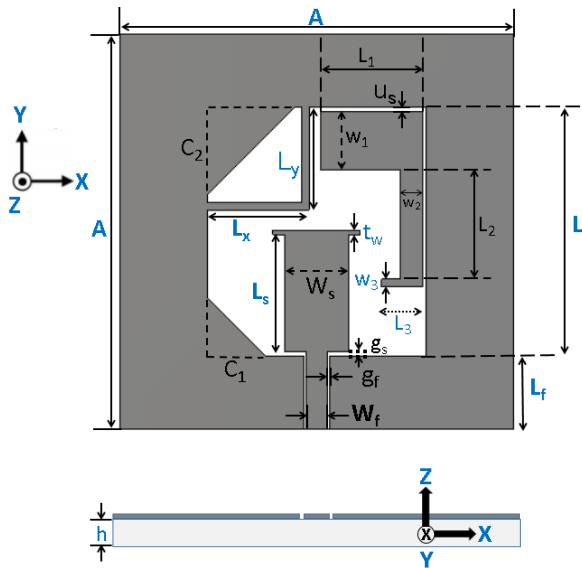


Fig. 1. Geometry of the proposed dual band CP slot antenna with CPW feed.

Two chamfered corners are used in the slot. The 1st one is at the lower left corner of the slot which helps to realize circular polarization at the higher frequencies. The 2nd one is located at the upper left corner of the slot and its dimension is optimized to be 12 mm, which is

close to the size of the inverted-L strip and this greatly enhances the circular polarized radiation at the 2.45 GHz resonant frequency. An asymmetric U-shaped strip is embedded near the upper right corner of the slot as a perturbed element. This asymmetric U-shaped strip is a key component to excite the required phase perturbation to produce a CP radiation [13]. It also generates the dual band operation of the antenna.

Table 1: Dimensions of the proposed antenna (unit: mm)

A	54	w_f	3
L	34	w_s	8.74
L_f	10	t_w	0.6
L_s	16	w_1	8
L_1	14	w_2	3
L_2	15	w_3	1
L_3	5.6	g_f	0.3
L_x	14	g_s	0.59
L_y	14	u_s	0.5
C_1	8	C_2	12

The extensive simulation trials illustrate that the inverted-L strip and the asymmetric U-shaped strip are key components to excite the required perturbation for a circular polarized radiation creation. There is a tradeoff between obtaining good impedance bandwidth ($|S_{11}| < -10 \text{ dB}$) and good axial ratio bandwidth ($AR < 3 \text{ dB}$). Therefore, optimization is used in order to achieve good performance in both the reflection coefficients and ARs. In order to design the proposed dual band CP slot antenna, the design optimization procedure is as follows:

- 1) Determine antenna size A and slot size L to adjust half wavelength resonator at 2.45 GHz.
- 2) Adjust the inverted-L strip and associated chamfered corner C_2 for axial ratio bandwidth (ARBW) at the lower band.
- 3) Adjust the asymmetric U-shaped strip and associated chamfered corner C_1 for impedance matching and ARBW at the higher band.
- 4) Perform impedance matching tuning using the protruded stub with its stepped impedance structure.
- 5) Slightly optimize the dimensions of the proposed antenna to achieve the desired dual band CP performance.

The antenna prototype is shown in Fig. 2. The reflection coefficients are obtained by simulation and measurement using Computer Simulation Technology Microwave Studio (CST MS) ver. 2017 and Agilent 8719ES vector network analyzer, respectively to validate the design. Two frequency bands of operation at 2.45 GHz and 5 GHz are observed in Fig. 3. The achieved frequency bands (for $|S_{11}| < -10 \text{ dB}$) are 1.73-2.64 GHz (with bandwidth of 910 MHz) for the IEEE 802.11b&g WLAN system, and 4.83-5.19 GHz (with bandwidth of

360 MHz) for the IEEE 802.11a/h/j/n/ac/ax WLAN system. The 2nd operating band covers different channels in the 5 GHz WLAN. These channels, according to the standard spectrum, are 7, 8, 9, 11, 12, 16, 34, 36, 38, 40, 42, 44, 183, 184, 185, 187, 188, 189, 192, and 196 [14].



Fig. 2. Photograph of the fabricated antenna.

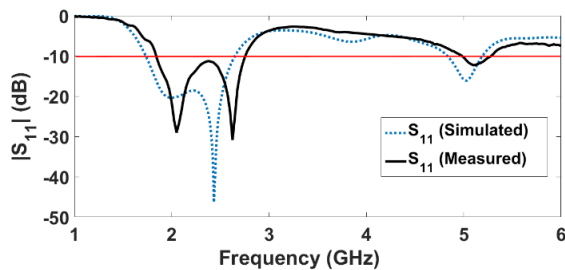


Fig. 3. Reflection coefficient of the proposed antenna.

The AR results also demonstrate the two operational bands at 2.45 GHz and at 5 GHz, respectively, as illustrated in Fig. 4. The achieved frequency bands (for AR < 3 dB) are 2.29-2.458 GHz (with bandwidth of 170 MHz) in the lower band, and 4.88-5.95 GHz (with bandwidth of 1.07 GHz) in the upper band. The measured values of the antenna axial ratio are 1.458 dB and 1.205 dB at 2.45 GHz and 5 GHz, respectively.

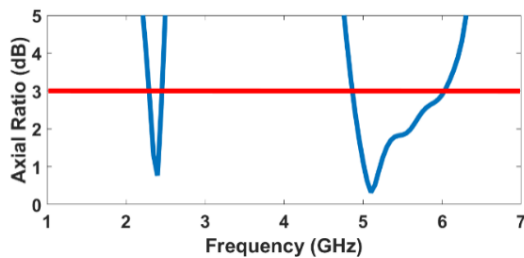


Fig. 4. Simulated axial ratio of the proposed antenna.

The designed antenna radiation patterns are examined by numerical simulations. The 3-D radiation pattern is shown in Fig. 5. In addition, measurement and simulation

results for both the E-plane and H-plane radiation characteristics are illustrated in Fig. 6. The antenna radiates in both front and back directions since all metal patches are printed on the top of the substrate. Also, at higher frequencies, the radiation patterns exhibit more rapid variations. The antenna gain variation is illustrated in Fig. 7. At 2.45 GHz, the achieved gain, directivity, and radiation efficiency are 3.74 dBi, 4.035 dBi, and 93.4%, respectively. At 5 GHz, the achieved gain, directivity, and radiation efficiency are 3.32 dBi, 4.09 dBi, and 83.7%, respectively.

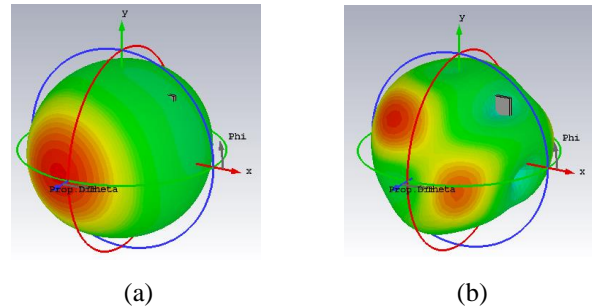


Fig. 5. 3-D radiation patterns of the proposed antenna at: (a) 2.45 GHz and (b) 5 GHz.

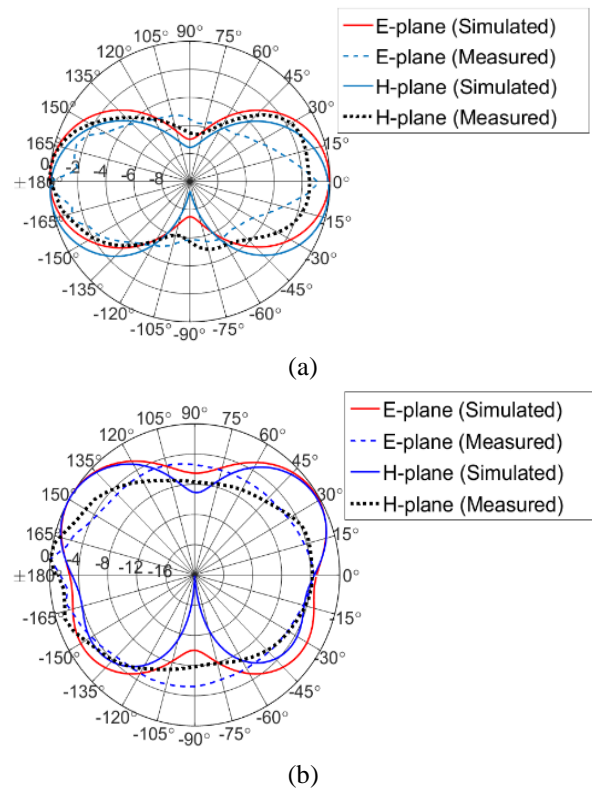


Fig. 6. Normalized radiation patterns of the proposed antenna at: (a) 2.45 GHz and (b) 5 GHz.

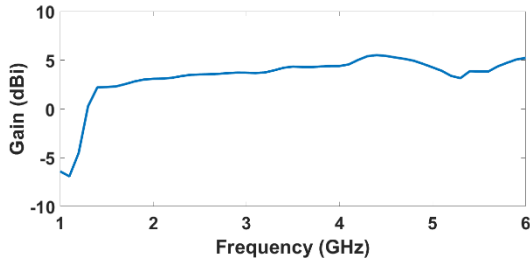


Fig. 7. Gain of the proposed antenna.

III. RECTIFYING CIRCUIT DESIGN

The structure of the rectifier consists of an impedance matching network, conversion circuit, and a resistive load. This can be illustrated from the block diagram of rectenna structure, shown in Fig. 8. The role of the impedance matching network is to maximize the power transfer from the receiving antenna to the conversion circuit. Then, the process of converting AC to DC signal is done. The topology of the conversion circuit used in this paper is the voltage doubler full wave rectification circuit and the Schottky diode HSMS-2860 is selected to be the rectifying device. Figure 9 illustrates the equivalent circuit model of the Schottky diode HSMS-2860. The most important component in the design of a rectifying circuit is the diode. Spice model parameters are taken from [15]. The diode turn on voltage V_T is 0.4 V and the reverse breakdown voltage V_{br} is 7 V. The series resistance R_s is 6 ohm and there is a variable junction resistance R_j in parallel with a junction capacitance C_j of 0.18 pF. The diode packaging leads to the emergence of the parasitic phenomenon that can be considered by a parasitic inductor of 2 nH and a parasitic capacitance of 0.08 pF.

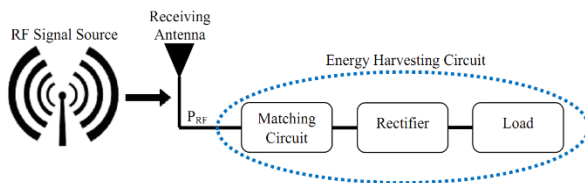


Fig. 8. Block diagram of rectenna structure.

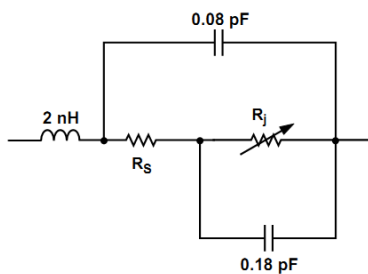


Fig. 9. Equivalent circuit model of the Schottky diode HSMS-2860 [13].

Before designing the impedance matching network, the input impedance of the voltage doubler circuit has to be calculated. This process has been done using the Advanced Design System (ADS) simulator and the real and imaginary parts of the input impedance at 0 dBm are illustrated in Fig. 10. At 2.45 GHz, the input impedance is $1.046 - j102.68 \Omega$, while at 5 GHz, the impedance is $1.142 - j34.1 \Omega$.

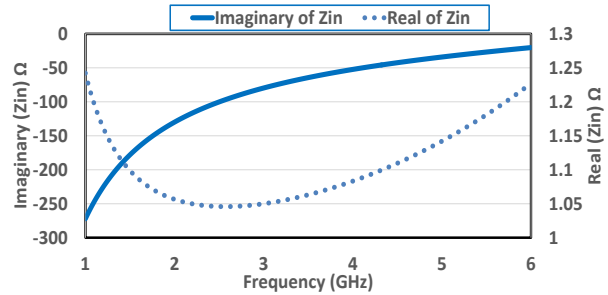


Fig. 10. Complex input impedance of the voltage doubler circuit at 0 dBm.

The impedance matching network is designed in order to match the receiving antenna with the rectifier at these two frequencies of operation, hence reduces power losses. Generally, lumped elements and distributed elements can be used for this purpose. In this paper, distributed elements are used in the form of Π -section configuration in order to achieve impedance matching at the two frequencies of operation. The lumped elements are not preferred due to their parasitics above 1 GHz and the limited available commercial values of these inductors and capacitors. According to [16], the Π section model has been used as a dual band impedance matching transformer for unequal complex impedance loads. The reflection coefficient of the matching network is shown in Fig. 11 and this proves the capability of the dual frequency matching circuit.

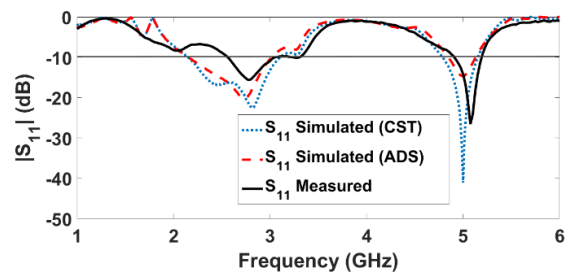


Fig. 11. Reflection coefficient of the matching network.

The geometry of the proposed dual band rectifier is illustrated in Fig. 12. The dimensions of the rectifier are $64 \times 28.8 \text{ mm}^2$. The distance between the voltage doubler circuit and the matching network is implemented in the form of a meander line for size reduction. Also, the tuning

stub is printed as an L-shaped stub for miniaturization. The characteristic impedance Z_c and the electrical length θ_c of the sections constituting the Π -model structure are initially calculated according to [16]. Then, the corresponding dimensions are optimized using ADS simulator, and the final dimensions are shown in Fig. 12.

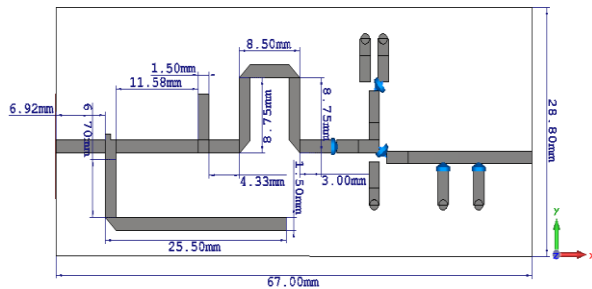


Fig. 12. Geometry of the proposed dual band rectifier.

Figure 13 illustrates the ADS simulation for both the voltage doubler circuit and the Π -model impedance matching circuit. The rectifier is fabricated on FR4 substrate with a dielectric constant of 4.3, thickness (h) of 0.8 mm, and loss tangent of 0.025. The total size of the rectifier is $64 \times 28.8 \times 0.8 \text{ mm}^3$. Figure 14 shows the photograph of the fabricated rectifier.

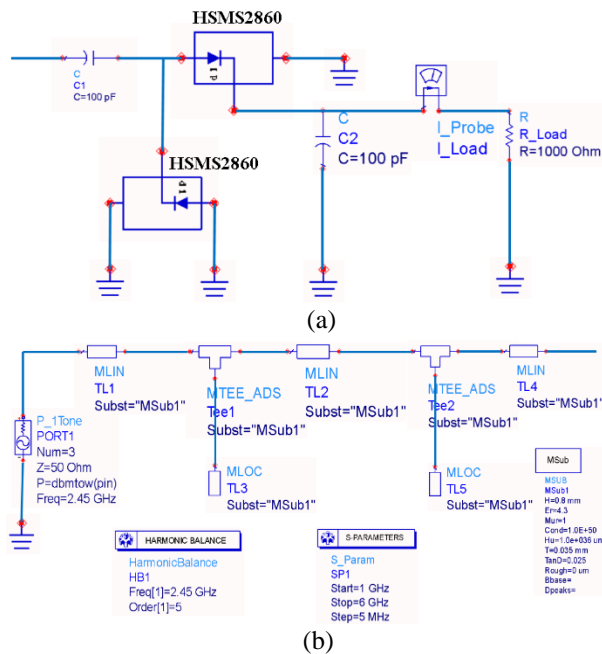


Fig. 13. ADS simulation for: (a) voltage doubler circuit, and (b) Π -model impedance matching circuit.

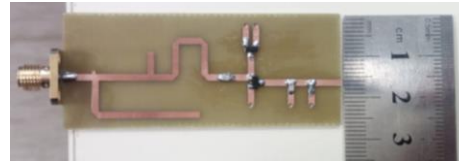


Fig. 14. Photograph of the fabricated rectifier.

Figure 15 shows the simulated and measured output voltage of the dual band rectifier as a function of the input power level when it is varied from -25 dBm to 15 dBm, and the load resistance is fixed at $1\text{K}\Omega$. For example, at 0 dBm, the simulated DC output voltage is 0.352 V at 2.45 GHz while it is 0.175 V at 5 GHz. The measured values are lower than the simulated ones. In addition, the power conversion efficiency is depicted in Fig. 16 for the dual frequency bands.

Different factors affect the conversion efficiency such as the diode turn on voltage, breakdown voltage, operating frequency, series resistance, and the load resistance [1]. The maximum simulated power conversion efficiency reaches 35.4% at 2.45 GHz and 20.9% at 5 GHz, at input power of 15 dBm. This may be due to the fact that the series resistance and the junction capacitance filter out much power as the frequency increases. Of course, the measured values are lower than the simulated ones.

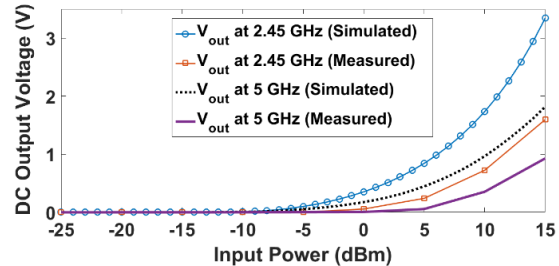


Fig. 15. Output voltage of the dual band rectifier.

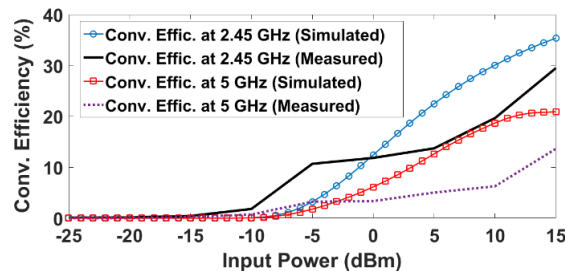


Fig. 16. Power conversion efficiency of the dual band rectifier.

IV. RECTENNA SYSTEM PERFORMANCE

The receiving antenna and rectifier are designed and evaluated separately. Then, they are assembled in order to complete the rectenna prototype which is fabricated and measured, as shown in Fig. 17. A 50 Ω adapter (SMA male-to-male) is used to connect the antenna to the rectifier since the antenna has copper metals on the top only due to the coplanar waveguide feeding, but the rectifier has top and bottom metal layers.

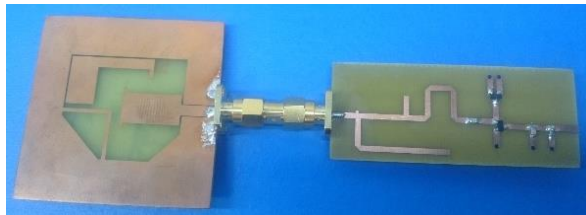


Fig. 17. Photograph of the fabricated rectenna.

The received RF power of antenna, P_{RF} , is measured by spectrum analyzer and the output voltage of rectenna (V_{out}) is measured by a voltmeter. The power conversion efficiency of rectenna η_{RF-DC} is defined as the ratio of the DC power P_{DC} and the RF power P_{RF} :

$$\eta_{RF-DC} = \frac{P_{DC}}{P_{RF}} \times 100\% = \frac{1}{P_{RF}} \times \frac{V_{out}^2}{R_{load}} \times 100\%. \quad (1)$$

The maximum measured conversion efficiency of the rectenna reaches 26.53% at 2.45 GHz and 12.74% at 5 GHz for an input power level of 15 dBm, as illustrated in Fig. 18. Table 2 shows the comparison between our designed rectenna and other designs reported previously in literature.

It can be seen that proposed design has advantages in the antenna impedance bandwidth and reduced dimensions compared to the circular polarized rectennas [7]. Compared to [11], compact size is achieved in the proposed rectenna. The proposed CP rectenna provides acceptable conversion efficiency as shown in the table and it is worth to note that the linear polarized rectenna cannot achieve constant DC power even if the received RF harvested signal has arbitrary polarization. This is a critical limit in most situations [3].

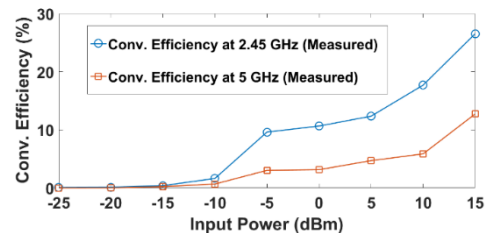


Fig. 18. Power conversion efficiency of the dual band rectenna.

Table 2: Comparison of the proposed rectenna and the related designs reported previously

Ref.	Freq. (GHz)	Ant. Dimensions (mm ³)	Max. Gain (dBi)	I/P Power Level for Peak η_{RF-DC} (dBm)	Max. η_{RF-DC} (%)	Polarization
[3]	2.39—2.52 and 5.65—5.85	44x41x1.6	5.53	10	45	Linear
[7]	0.908—0.922 and 2.35—2.5	120x120x8.67	6.14	0 to 5	39	Circular
[11]	0.88—8.45	100x100x1.6	8.7	-5 to 0	51.8	Linear
This work	1.73—2.64 and 4.83—5.19	54x54x1.6	5.51	5 to 10	35.4	Circular

V. CONCLUSION

This paper presented a dual band rectenna operating at the two WLAN frequency bands 2.45 GHz and 5 GHz. The receiving slot antenna is a dual band CP CPW feed with only one feeding port. The antenna dimensions are $54 \times 54 \times 1.6$ mm³ with the metal deposited only on one side of the substrate. The proposed antenna -10 dB bandwidth extended from 1.73 GHz to 2.64 GHz for the 1st band and from 4.83 GHz to 5.19 GHz for the 2nd band. The ARBW (for AR < 3 dB) extended from 2.29 to 2.458 GHz (with bandwidth of 170 MHz), and from 4.88 to 5.95 GHz (with bandwidth of 1.07 GHz) for 1st and 2nd

bands, respectively. A dual band voltage doubler rectifier has been designed based on a Π -model impedance transformer for dual band operation. The rectifier dimensions are $64 \times 28.8 \times 0.8$ mm³. The prototypes of the proposed antenna and rectifier were fabricated and measured. Good agreement was found between measured and simulated reflection coefficients. The proposed rectenna is integrated. PCE is measured at different input power levels. An efficiency of 26.53% and 12.74% are achieved at 2.45 and 5 GHz frequencies, respectively. The proposed rectenna has an advantage of obtaining constant DC power at random polarization angles which

makes it suitable for ambient RF energy harvesting applications for powering wireless sensors in various IoT applications.

ACKNOWLEDGMENT

This work is funded by the National Telecom. Regulatory Authority (NTRA), Ministry of Communications and Information Technology (MCIT), Egypt.

REFERENCES

- [1] C. R. Valenta and G. D. Durgin, "Harvesting wireless power: Survey of energy-harvester conversion efficiency in far-field, wireless power transfer systems," *IEEE Microw. Mag.*, vol. 15, no. 4, pp. 108-120, June 2014.
- [2] H. Sun and W. Geyi, "A new rectenna with all-polarization-receiving capability for wireless power transmission," *IEEE Antennas and Wireless Propagation Letters*, vol. 15, pp. 814-817, 2016.
- [3] O. Amjad, S. W. Munir, Ş. T. İmeci, and A. Ö. Ercan, "Design and implementation of dual band microstrip patch antenna for WLAN energy harvesting system," *Applied Computational Electromagnetics Society Journal*, vol. 33, no. 7, pp. 746-751, July 2018.
- [4] A. Khemar, A. Kacha, H. Takhedmit, and G. Abib, "Design and experiments of a dual-band rectenna for ambient RF energy harvesting in urban environments," *IET Microwaves, Antennas & Propagation*, vol. 12, no. 1, pp. 49-55, 2018.
- [5] K. Dey, T. Dey, R. Hussain, and A. Eroglu, "Design of dual band rectifiers for energy harvesting applications," *2018 International Applied Computational Electromagnetics Society Symposium (ACES)*, Denver, CO, 2018, pp. 1-2.
- [6] M. Mattsson, C. I. Kolitsidas, and B. L. G. Jonsson, "Dual-band dual polarized full-wave rectenna based on differential field sampling," *IEEE Antennas and Wireless Propagation Letters*, vol. 17, no. 6, pp. 956-959, June 2018.
- [7] A. M. Jie, N. Nasimuddin, M. F. Karim, and K. T. Chandrasekaran, "A dual-band efficient circularly polarized rectenna for RF energy harvesting systems," *Int. J. RF Microw. Comput. Aided Eng.*, vol. 29, pp. 1-11, Jan. 2019.
- [8] E. Liu, X. Yang, and L. Li, "Triple-band GCPW rectifier for harvesting EM energy," *2017 International Applied Computational Electromagnetics Society Symposium (ACES)*, Suzhou, 2017, pp. 1-2.
- [9] S. Chandravanshi, S. S. Sarma, and M. J. Akhtar, "Design of triple band differential rectenna for RF energy harvesting," *IEEE Transactions on Antennas and Propagation*, vol. 66, no. 6, pp. 2716-2726, June 2018.
- [10] N. Singh, B. K. Kanaujia, M. T. Beg, Mainuddin, T. Khan, and S. Kumar, "A dual polarized multi-band rectenna for RF energy harvesting," *AEU - International Journal of Electronics and Communications*, vol. 93, pp. 123-131, 2018.
- [11] X. Bai, J. Zhang, L. Xu, and B. Zhao, "A broadband CPW fractal antenna for RF energy harvesting," *Applied Computational Electromagnetics Society Journal*, vol. 33, no. 5, pp. 482-487, May 2018.
- [12] M. Shokri, S. Asiaban, and Z. Amiri, "Study, design and fabrication of a CPW fed compact monopole antenna with circular polarization for ultra wide band systems application," *Applied Computational Electromagnetics Society Journal*, vol. 32, no. 9, pp. 749-753, Sept. 2017.
- [13] W. C. Weng, J. Y. Sze, and C. F. Chen, "A dual-broadband circularly polarized slot antenna for WLAN applications," *IEEE Transactions on Antennas and Propagation*, vol. 62, no. 5, pp. 2837-2841, May 2014.
- [14] En.wikipedia.org. List of WLAN channels. [Online] Available at: https://en.wikipedia.org/wiki/List_of_WLAN_channels [Accessed 1 July 2018].
- [15] Hewlett-Packard Co., "Surface mount microwave schottky detector diodes," 5968-4188E datasheet, 1999.
- [16] O. Manoochehri, A. Asoodeh, and K. Forooghi, "PI-Model dual-band impedance transformer for unequal complex impedance loads," *IEEE Microwave and Wireless Components Letters*, vol. 25, no. 4, pp. 238-240, Apr. 2015.